

VALIDATION OF SPH PREDICTIONS OF OXIDE GENERATED DURING AL MELT TRANSFER

Mahesh PRAKASH^{1*}, Gerald G. PEREIRA¹, Paul W. CLEARY¹, Patrick ROHAN² and John A. TAYLOR³

CAST Cooperative Research Centre (CAST)

¹CSIRO Mathematical and Information Sciences, Private Bag 33, Clayton, Victoria 3169, AUSTRALIA

²CSIRO Materials Science and Engineering, Private Bag 33, Clayton, Victoria 3169, AUSTRALIA

³School of Mechanical and Mining Engineering, The University of Queensland, Brisbane, QLD 4074, AUSTRALIA

*Corresponding author, E-mail address: Mahesh.Prakash@csiro.au

ABSTRACT

Aluminium melt transfer operations can lead to significant amounts of dross formation. A significant proportion of this metal loss may be prevented by adopting more efficient melt transfer strategies that reduce splashing and turbulence thereby resulting in reduced oxide and therefore dross formation. Optimisation of such systems can be achieved rapidly by employing computational modelling to explore the effects of changed conditions such as crucible tilt speed, spout height and spout geometry. From a modelling perspective, accurately predicting the amount of oxide produced during melt transfer operations is difficult due to the inability of existing mesh-based flow modelling techniques to carry history information such as mass of oxide formed on a per node basis. Difficulty also arises due to the lack of validated oxidation models useful for such flow regimes. The grid-free Smoothed Particle Hydrodynamics (SPH) method has been used to predict the amount of oxide generated during a molten metal transfer process, where the metal is poured into a sow from a tilting crucible furnace. The Lagrangian framework allows tracking of history-dependent properties such as accumulated oxide mass. An oxidation model based on skimming trials performed at the laboratory scale is used. Favourable comparisons with experimentally measured oxide levels are obtained for metal transfer rates from 0.8 – 5.2 kg/s.

INTRODUCTION

Aluminium melt transfer operations can lead to significant amounts of dross formation. A significant proportion of this metal loss may be prevented by adopting more efficient melt transfer strategies that reduce splashing and turbulence thereby resulting in reduced oxide and therefore dross formation. Clark and McGlade (2005) conducted a survey of the Australian and New Zealand primary aluminium smelters and found that amongst casthouse practitioners it was generally accepted that 80% of casthouse melt losses occurred within the casting furnace, and that 60% of those losses were generated during furnace filling procedures, typically “cascading” events (Figure 1). For the case of processing 50 t of primary aluminium and assuming a typical 1% dross level formed during processing (i.e. 500 kg), then according to these survey results, 240 kg (or 48% of the total dross) would result directly from the furnace filling activity. Further, assuming all the dross formation resulted from the full conversion of liquid Al to oxide, this represents a

net loss of 127 kg of metallic Al and a net weight gain of 113 kg due to oxygen uptake. Since the dross is likely to contain a proportion of unrecovered metal, the above calculation will be a mild over-estimate.

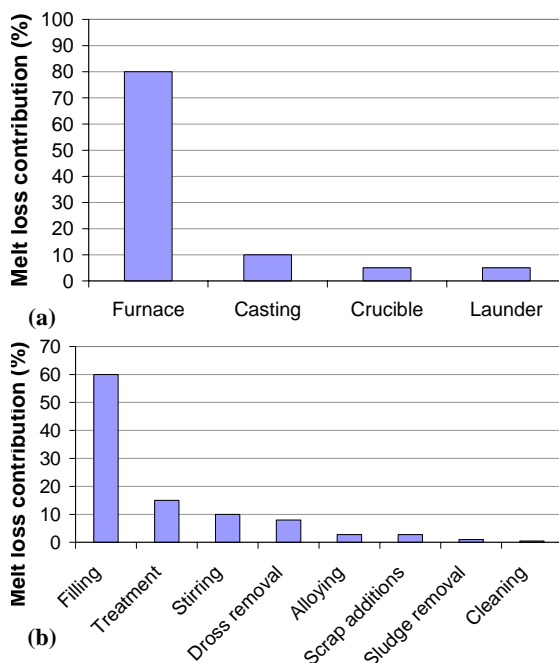


Figure 1: Estimated breakdown of (a) melt losses occurring within a primary Al casthouse and (b) furnace-based melt losses, Clark and McGlade (2005).

This calculation demonstrates the importance of reducing melt loss in the Al industry. A recent overview of oxidation of Al, dross formation and melt losses in Al smelter casthouses can be found in Taylor (2007).

SPH is a grid-free flow modelling method that has specific advantages over mesh-based techniques for simulating Al melt transfer operations including:

- Simulation of highly transient and complex free surface flows;
- The Lagrangian framework of the method allows tracking of history-dependent properties such as accumulated oxide mass;
- Complex moving parts often encountered in melt transfer operations can be modelled easily.

A review of the method can be found in Monaghan (1992, 1994) and a review of its industrial applications can be

found in Cleary et al. (2007). The method has been previously used for several Al casting related applications such as HPDC (Ha and Cleary, 2000 and Cleary et al., 2006); LPDC (Cleary 2008) and gravity die casting (Ha et al. 2000). In Al ingot casting it has been used to optimize the casting wheel design by reducing the oxide generated by about 50% and at the same time increasing the throughput by 50% compared to existing industrial designs (Prakash et al. 2007).

CAST CRC is working to understand oxide formation during melt pouring events with the ultimate aim of developing novel technologies to minimize dross formation and melt loss. The project involves several aspects, of which the SPH modelling and related experimental aspects are presented here. These involve:

- Establishing reliable oxidation rates for molten aluminium exposed to air;
- Building a medium-scale (500 kg max) instrumented melt transfer rig capable of detecting the expected weight gains associated with oxidation during a turbulent pouring event;
- Developing a modelling method that can predict oxide formation on flowing melts;
- Validating the model against experimental data;
- Using the modelling methodology to simulate complex industrial-scale problems and to develop appropriate solutions.

DEVELOPMENT OF THE OXIDE MODEL

Following a survey of experimental methods used for measuring oxidation rates of molten metal, it was decided to adopt the technique used and partially-described by Freti et al. (1982). This involved constructing a bath with a high surface to volume ratio (shown in Figure 2) that could hold molten aluminium at a constant temperature. The oxide skin generated was skimmed at time intervals ranging from a few seconds to several hours. The molten surface was fully exposed to ambient air. The skimming blade produces a folded skin of oxide with entrapped metal that is removed immediately and cooled to prevent further oxidation. Typically 10 skims, each of 0.5 m², were collected for shorter exposure times (up to 1 hr) since oxidation rates are the highest at early times and these are most relevant to the current study. Fewer samples were taken for longer intervals since the oxidation rate did not seem to vary significantly after around 1 hr.



Figure 2: Oxide skim is collected from skimming rig by pulling a blade across the melt surface at regular intervals.

These skims were weighed and analysed for metal content using a specifically-formulated molten salt mix to separate the oxide from the aluminium. The molten salt mixture was then chill solidified, the crystallised salt dissolved away in warm water and the metallic residue was dried

and weighed. The difference between the original skim weight and the recovered aluminium weight gives the amount of oxide formed for a given exposed surface area for that exposure duration. This gives the oxidation rate as a function of time.

The experimental data obtained for commercially pure Al (>99.7%) at controlled melt temperatures between 750 and 850°C yielded a general equation for overall oxidation rate, OOR, versus exposure time, t , of the power law type (equation 1), where a and b are fitting constants derived from the best straight line fit on a log-log plot. The effect of temperature can be largely ignored in this case, giving the temperature-independent equation:

$$\text{OOR} = a \cdot t^{-b} \text{ gm}^{-2} \text{ s}^{-1} \quad (1)$$

For this equation to be useful for making predictions of oxidation occurring at short time scales, it was necessary to extrapolate the relationship to much shorter times (i.e. small fractions of a second) than were possible for experimental data collection. This shorter-time scale data was estimated from calculated oxidation rates for fine-scale aluminium powder particles of various sizes based on their measured oxygen content and known production parameters (Locatelli, 2008). The estimates were compared against linear extrapolations at short time scales using equation (1) and resulted in a very good fit.

CRUCIBLE POURING EXPERIMENTS

A 500 kg tilting crucible furnace was used to estimate oxidation in medium-scale cascading events. A sow mould capable of holding the same amount of Al was used to receive the metal. Three high sensitivity load cells were installed under the tilting crucible frame, and a single load cell was placed to measure the weight in the sow mould. These four load cells were connected to a PC. The equipment setup is shown in Figure 3.



Figure 3: 500 kg tilting furnace and slung sow used for crucible pouring experiments.

Using static and transferred solid weights, it was established that the best accuracy expected during a liquid pouring trial was approx. ± 50 g across the whole pouring system. Real-time measurement was not possible (due to errors induced by furnace and sow mould movements) so only the static start and finish measurements are used here.

Aluminium ingots (99.7% purity) were charged into the crucible furnace and melted. The coated sow mould was

pre-heated in an oven to 500°C (to prevent premature solidification of the transferred metal). When the melt temperature was stabilized, the heated sow mould was moved into position and suspended from the sling. Once load cell outputs had settled and start weights recorded, pouring commenced. When a transfer was complete, the furnace was returned to the fully down position, the sow was steadied, and the finish weights for the furnace and sow were recorded. The sow was then skimmed in order to remove and collect the accumulated dross for future reference and analysis.

These pouring (cascading transfer) trials produced no measurable weight gains across the full range of testing conditions. This implied that the amounts of oxide produced were actually quite small, i.e. below our minimum detection level of ~50 g (via weight gain measurements). The use of a weight gain technique to measure oxide levels is therefore not recommended especially when purity aluminium is used.

Analysis was therefore performed on the dross skims collected to chemically estimate the amount of oxide present. Most collected skims were approx. 0.5 – 1 kg total mass. The results indicated that the skim samples were 96 - 97% metallic content (compared to 30 - 80% Al content typical in industrial dross) and that therefore they each only contained 15 – 45 g of actual aluminium oxide. This amount of oxide (and its associated mass gain) was below the detection limit of the experimental set-up using weight gain as a measure of oxide generated. It was also 1 to 2 orders of magnitude less than expected. The next step was to ascertain the amount of oxide formation that would be predicted for these experimental test cases using SPH.

SPH MODELLING APPROACH

SPH is a Lagrangian (grid-free) computational method for modelling heat and mass flow and is well suited to simulating free surface flows such as molten metal transfer. In SPH, materials are approximated by particles that are free to move around rather than by fixed grids or meshes. The particles are moving interpolation points that carry with them physical properties, such as the mass of the fluid, its temperature, enthalpy, density and any other relevant properties, such as the degree of oxidation. Boundaries such as the crucible and the sow are modelled using SPH particles at which a Lennard-Jones type penalty force is applied in the normal direction. The boundary particles are included in the calculations of the viscous stress to produce a non-slip boundary condition for the fluid. These boundary particles can move either due to a prescribed behaviour such as the crucible or can move dynamically due to fluid and other forces. Comprehensive details on the SPH method can be found in Monaghan (1992, 1994) and Cleary et al. (2007).

The initial simulation setup is shown in Figure 4. The furnace is filled with metal (coloured blue) and the sow is initially empty. The red circle at the tip of the crucible is the pivot about which the crucible rotates. The SPH particle spacing was determined after a resolution analysis to ensure that the oxide levels predicted did not change with a change in the fluid and boundary particle spacing. An SPH resolution of 12 mm was used for all solid and liquid components.

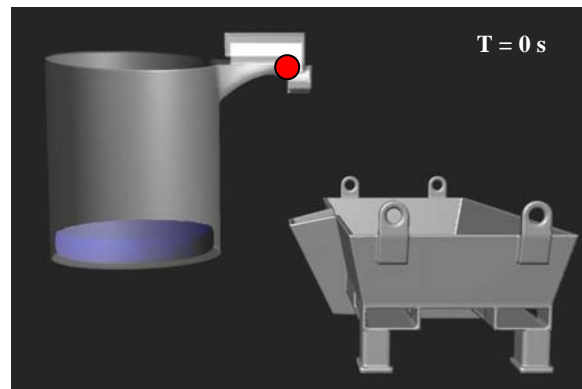


Figure 4: SPH representation of tilting furnace and sow. Molten Al (blue) is initially in the crucible furnace.

The SPH modelling technique keeps track of the oxide that is created whenever a particle is exposed to air. The Al particles are initially free of oxide. While exposed at a melt surface, they oxidise and the cumulative oxide is calculated. The oxidation model applied to the SPH simulations is the power law relationship in equation 1. SPH is therefore able to predict the distribution and total amount of oxide formed.

FLOW OF AL FROM CRUCIBLE TO SOW

Figure 5 shows the pouring of molten Al from the crucible furnace into the sow at the highest transfer rate used in the experiment. It is coloured by velocity with blue being 0 m/s and red being 2 m/s. This case has 76 kg of molten Al transferred at a rate of 5.26 kg/s from a fall height of 720 mm (measured from the rotation pivot of the crucible to the base of the sow). By 10 s, the crucible has rotated by 62°. The entire metal mass is still in the furnace with the fluid just starting to collect close to the lip of the crucible. At 13 s, the metal starts pouring into the deep central section of the sow with a velocity of more than 2 m/s. It shows significant fragmentation and splashing with some metal spilling out of the sow. This behaviour was also observed during the experiments for high metal transfer rates. At 15 s, the central section of the sow is almost completely filled. Further splashing of the metal out of the sow is seen. The intense fragmentation of the metal during this pouring phase is expected to result in significant fresh free surface creation thereby leading to high rates of oxide formation. At 16 s, the metal starts filling the shallow sections on either side of the sow after completely filling the central deep section. The intense splashing of the metal has stopped now due to the presence of the central pool into which additional metal is poured. At 17 s, the metal from the crucible has been fully emptied into the sow. The metal in the sow sloshes back and forth creating additional free surface and higher oxide growth. This oxide forms at a slower rate than the pouring stage. At 20 s, the sloshing motion has reduced significantly but the central section is still moving gently. After 20 s, the growth of oxide continues at a more moderate rate due to the gently moving liquid metal in the sow.

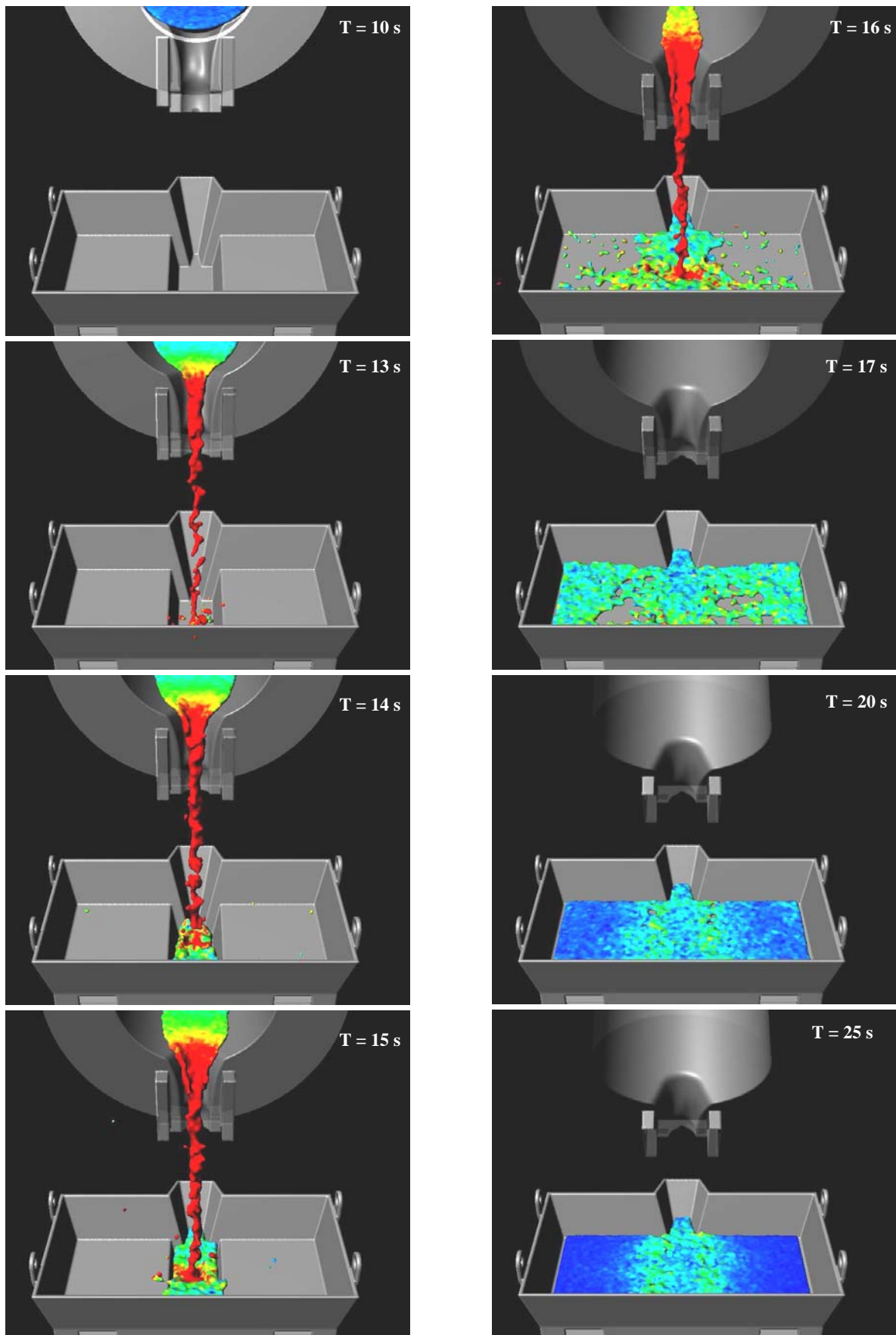


Figure 5: SPH prediction of metal transfer from furnace to sow. The metal is coloured by velocity. Blue = 0 m/s and red = 2 m/s. The conditions are: 720 mm fall height, 5.25 kg/s pouring rate and total metal transfer of 76 kg.

POURING TRIALS AND OXIDE GENERATED

Table 1 shows the range of crucible pouring trials conducted experimentally and simulated using SPH. Two different fall heights of 720 and 920 mm were used. The metal pouring rate was varied from 0.8 to 5.2 kg/s so as to assess its effect on the variation in oxide generated. The amount of metal poured was 80 kg for each pouring trial. The amount of oxide generated in the simulations, using the conditions in Table 1 is shown in Figure 6 for the 720 and 920 mm fall heights. In each case the oxide formation has three distinct stages:

- i. Slow oxidation of the melt surface exposed during the initial tilting of the furnace, before the melt starts to cascade;
- ii. Rapid oxide formation during the cascading flow of metal from furnace to sow;
- iii. Lower oxidation rate after pouring is complete and the metal surface gradually settles in the sow. Oxidation never stops, but starts to plateau out at this stage.

The predicted oxide is compared with the corresponding experimental data from the pouring rig in Figure 7 (i.e. from the collected dross skims analysed for metal/oxide content). The SPH oxide mass predictions are of a similar order of magnitude to those obtained experimentally for fall heights of 720 and 920 mm.

The simulated oxide levels are on average 43% (range 27-54%) lower than the experimentally measured oxide. This is mainly because the simulations end when the melt is judged to have become quiescent and do not attempt to model the complex act of collecting the dross skims from the melt. This collection process can involve several passes with the skimming tool and can result in the generation of a large amount of fresh molten Al surface that re-oxidizes, thus increasing the amount of oxide present. In addition, the collected skims may contain significant levels of entrapped metal which when removed from the melt as dross may be subject to further oxidation until the skimmed mass finally solidifies.

The difference between the prediction and experimental data is consistently smaller for the higher fall height of 920 mm being 38% lower on average compared to 48% lower on average for a fall height of 720 mm. This could be because for the higher fall height a larger proportion of the oxide is formed due to the actual pouring event compared to events occurring downstream such as skimming.

Both the simulated and experimental values are much smaller than indicated by industrial expectations. Cascading events certainly generate a significant amount of fresh metal surface area (the SPH simulations provide this information) but the oxide that forms on this new surface, although rapid, is actually very thin and only amounts to a small mass. If this is scaled-up pro rata for industrial-sized crucibles of 5 t capacity, then the amount of oxide predicted for say 10 sequential pours (to fill a 50 t furnace) is more than an order of magnitude less than is estimated from the large amount of dross skimmed and weighed following a 2-3 hour furnace preparation regime.

So although cascading is detrimental, the present work suggests that the actual physical process of “cascade” pouring several crucibles into a furnace is unlikely to be the most significant oxide contributor to dross generation.

Most furnace filling scenarios (even those using siphoning techniques) involve short term filling activity followed by prolonged periods of exposure of melt baths to air between crucible transfers. This exposure involves several different aspects that have not been explored to date and which may eventually account for the large discrepancy noted above such as:

- i. Large molten metal surface area within a quiescent furnace with normally-growing oxide skin. This could contribute significantly more to the overall oxide compared to the smaller surface area in the sow in the current experimental setup;
- ii. Patches of oxide skin that have developed breakaway oxidation characteristics over time. Breakaway oxidation occurs when the oxide skin is very long-lived and gets heated up to excessively high temperatures resulting in significantly higher oxidation rates;
- iii. Regions of convoluted, folded oxide skins that form during each transfer event which float and drift around the melt surface as “islands”. These “islands” have entrapped air and fresh metal and therefore are subject to further oxidation;
- iv. High near-surface temperatures (and sometimes complex atmospheres) in operating furnaces, compared to constant source of ambient fresh air above the experimental test rig melt surfaces. These conditions can contribute to an earlier onset of breakaway oxidation.

No:	Fall height (mm)	Pour rate (kg/s)	Metal mass (kg)
1	720	0.86	77
2	720	1.35	77
3	720	2.62	90
4	720	5.26	76
5	920	0.80	77
6	920	0.90	77
7	920	2.08	77
8	920	3.59	77

Table 1: Conditions used for crucible pour experiments and simulations.

CONCLUSION AND FUTURE DIRECTIONS

Initial indications are that a useful oxidation rate has been developed which when used in conjunction with SPH is capable of predicting the approximate amount of oxide that is generated in a simple, single, medium-scale pouring event in the laboratory. It is clear however, that the oxide model needs to be further improved in order for it to be able to predict dross levels in industrial furnace situations.

These improvements will be in the form of including the effects of melt temperature, alloy composition and furnace atmosphere into the oxidation model. It is also intended that the SPH results will be improved by the incorporation of greater detail and resolution of the plunge/splash region where the metal stream impacts the bath. Further medium-scale pouring trials will be required to validate the predictive capability of such changes.

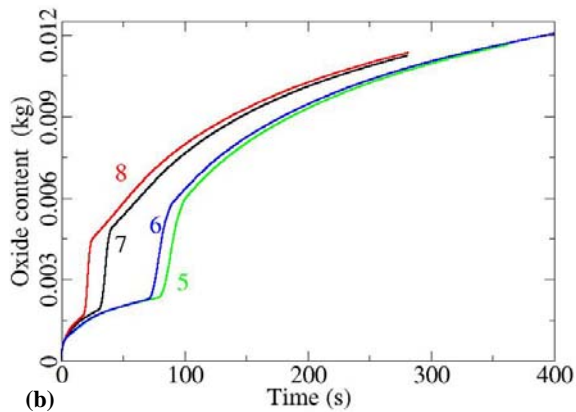
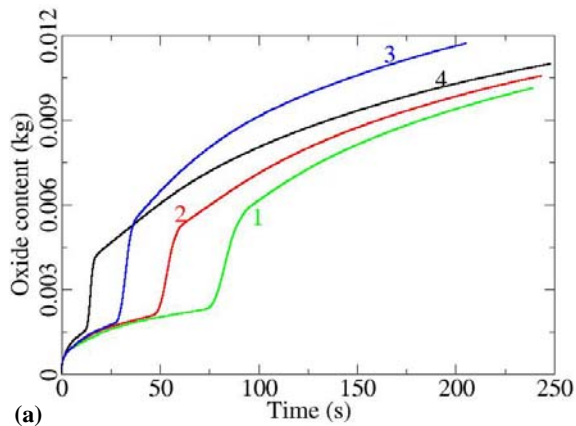


Figure 6: Predicted oxide mass (kg) versus time for fall heights of (a) 720, and (b) 920 mm for sow weight pours of ~80 kg. The trial numbers are given in Table 1.

ACKNOWLEDGMENTS

CAST CRC is established under and is funded in part by the Australian federal governments co-operative research centres scheme. Rio Tinto Alcan is a core member of the CAST CRC and their support is gratefully acknowledged.

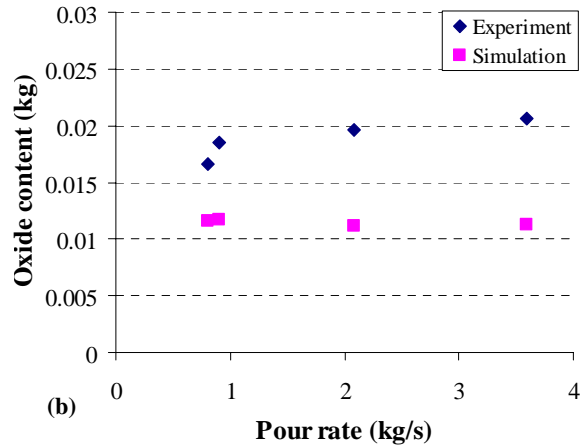
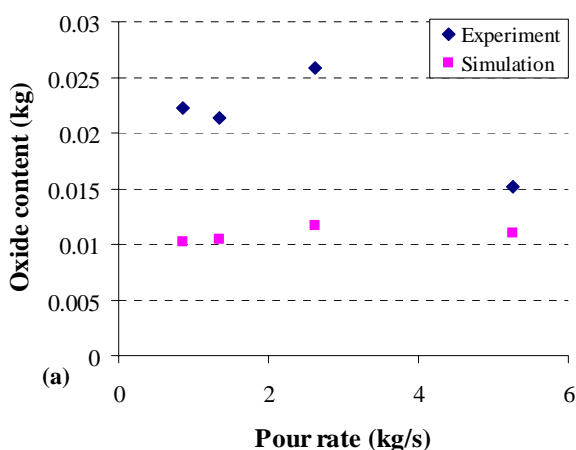


Figure 7: Oxide content (SPH-predicted and experimental) versus cast rate for pouring trials at (a) 720 mm and (b) 920 mm fall height.

REFERENCES

- CLARK, A. and McGLADE, P. (2005), "Furnace dross prevention, melt loss reduction and dross recycling: Review of best practice," *3rd Int. Melt Quality Workshop*, Dubai, UAE, 14-16th November, 8 pp.
- CLEARY, P. W., HA, J., PRAKASH, M. and NGUYEN, T., (2006), "3D SPH Flow Predictions and Validation for High Pressure Die Casting of Automotive Components", *App. Math. Model.*, **30**, 1406-1427.
- CLEARY, P. W., PRAKASH, M., HA, J., STOKES, N., and SCOTT, C., (2007), "Smooth Particle Hydrodynamics: Status and future potential", *Progress in Computational Fluid Dynamics*, **7(2-4)**, 70-90.
- CLEARY, P., (2008), "Prediction of feeding, freezing and defect creation in low pressure die casting", *Proc. of 6th Int. Conf. on CFD in Oil & Gas, Metallurgical and Process Industries*, Trondheim NORWAY, 10-12 June.
- FRETI, S., BORNAND, J. D. and BUXMANN K., (1982), "Metallurgy of dross formation on aluminium melts," *Light Metals 1982* (Warrendale, PA: TMS, 1982), 1003-1016.
- HA, J. and CLEARY, P. W., (2000), "Comparison of SPH simulations of high pressure die casting with the experiments and VOF simulations of Schmid and Klein", *Int. J. Cast Metals Research*, **12**, 409-418.
- HA, J., SCHUHMANN, R., ALGUINE, V., CLEARY, P. and NGUYEN, T., (2000), "Real-time Xray imaging and numerical simulation of die filling in gravity die casting", *Proc. Modelling of Casting, Welding and Advanced Solidification Processes IX*, 151-158.
- LOCATELLI, J., (2008), Private communication with author, Unpublished industry data.
- MONAGHAN, J. J., (1992), "Smoothed particle hydrodynamics", *Annual Review of Astronomy and Astrophysics*, **30**, 543-574.
- MONAGHAN, J. J., (1994), "Simulating free surface flows with SPH", *J. Comp. Physics*, **110**, 399-406.
- PRAKASH, M., CLEARY, P. W., GRANDFIELD, J., ROHAN, P. and NGUYEN, V. (2007), "Optimisation of ingot casting wheel design using SPH simulations.", *Prog. in Computational Fluid Dynamics*, **7(2-4)**, 101-110.
- TAYLOR, J. A., (2007), "Oxidation, dross and melt loss issues involved in the aluminium cast house," *Proc. 10th Australasian Conference on Aluminium Cast House Technology*, Sydney, 6-9th August, 47-55.